Nanoscale

# Electrostatics of DNA Nucleotides-Carbon Nanotube Hybrids Evaluated From QM:MM Simulations



| | |
|---|---|
| Journal: | *Nanoscale* |
| Manuscript ID | NR-ART-06-2015-003665.R1 |
| Article Type: | Paper |
| Date Submitted by the Author: | 09-Sep-2015 |
| Complete List of Authors: | Chehel Amirani, Morteza; University of Alberta, Mechanical Engineering<br>Tang, Tian; University of Alberta, Mechanical Engineering |
| | |

# Electrostatics of DNA Nucleotides-Carbon Nanotube Hybrids Evaluated From QM:MM Simulations

Morteza Chehel Amirani and Tian Tang*

*Department of Mechanical Engineering, University of Alberta, Edmonton, AB, Canada*

E-mail: tian.tang@ualberta.ca

*To whom correspondence should be addressed

**Abstract**

Biomolecule-functionalized carbon nanotubes (CNTs) have been studied vastly in recent years due to their potential applications for instance in cancer detection, purification and separation of CNTs, and nanoelectronics. Studying the electrostatic potential generated by a biomolecule-CNT hybrid is important in predicting its interactions with surrounding environment such as charged particles and surfaces. In this paper, we performed atomistic simulations using a QM:MM approach to evaluate the electrostatic potential and charge transfer for a hybrid structure formed by a DNA nucleotide and a CNT in solution. Four types of DNA nucleotides and two CNTs with the chiralities of (4,4) and (7,0) were considered. The type of the nucleotide and CNT were both found to play important role in the electrostatic potential and charge transfer of the hybrid. At the same distance from the CNT axis, the electrostatic potential for the nucleotides-(4,4) CNT hybrids was found to be stronger compared with that for the nucleotide-(7,0) hybrids. Higher electric charge was also shown to be transferred from the DNA nucleotides to the (7,0) CNT compared with the (4,4) CNT. These results correlate with the previous finding that the nucleotides bound more tightly to the (7,0) CNT compared with the (4,4) CNT.

*Keywords*: DNA, Nucleotide; Carbon nanotube; Electrostatic potential; Charge transfer; QM:MM

# 1 Introduction

Hybrids formed by DNA and carbon nanotube (CNT) have attracted much attention in recent years due to their interesting properties and useful applications.[1–7] Dispersion and separation of CNTs using single stranded DNA (ssDNA) is one such application. Due to the hydrophobic nature of CNT, its dispersion in water is difficult and bundled CNTs are usually formed in aqueous solution.[8] Some methods have been proposed to increase the solubility, but they may alter some of CNT's properties at the same time. For example, shortening CNTs using acids can increase their solubility, but meanwhile this reduces the aspect ratio of the CNTs.[9,10] In addition to the poor solubility, separation of CNTs according to their chirality is another challenge in their synthesis, which is critical in electronic applications where the CNT's electric properties play an important role. In an experiment by Zheng *et al.*,[1] ssDNA was found to helically wrap around the CNT and form a hybrid structure in an electrolyte solution. The negatively charged phosphate groups in the ssDNA backbone caused the hybrids to repel, leading to a stable solution of dispersed hybrids. Separation of the CNTs into metallic and semiconducting types was subsequently achieved using the method of ion exchange chromatography (IEC). In the IEC, the negatively charged hybrids were adsorbed on the positively charged IEC column. With increasing salt concentration, it was found the ssDNA-metallic CNT hybrids generally desorb earlier from the column than the ssDNA-semiconducting CNT hybrids, allowing for their separation. The separation was shown to strongly depend on the ssDNA sequence.[11,12] More recently, separation of semiconducting CNTs with the same diameter but different chiralities (e.g. (9,1) and (6,5)) has been successfully carried out.[13,14]

Several attempts have been put forward in order to understand the mechanism of the separation phenomenon. Zheng *et al.* proposed that ssDNA sequence and electronic properties of the CNT influence the surface charge of the CNT hybrid.[1] Based on a free energy formulation,[15] they predicted ssDNA-metallic CNT to possess less surface charge and hence less binding strength to the IEC column than the ssDNA-semiconducting CNT, if the same ssDNA is used. Khripin *et al.* evaluated the mobility of poly$(GT)_{30}$ ssDNA-CNT hybrids using capillary electrophoresis (CE) technique.[16] With the measured mobility and making use of the Poisson-Boltzmann (PB) equa-

tion and electric double layer formulation,[17] they obtained different average charge densities for ssDNA-(6,5) CNT and ssDNA-CNT (7,5) hybrids: -6.0 $e/nm$ for the former and -6.8 $e/nm$ for the latter. They also performed molecular dynamics (MD) simulations to obtain optimized structure of the ssDNA on different CNTs. Based on the wrapping angle, the charge of the hybrid per unit length of the CNT was determined to be -5.8 $e/nm$ and -6.2 $e/nm$, respectively for ssDNA-(6,5) CNT and ssDNA-CNT (7,5) hybrids. Although these values were in good agreement with those calculated based on CE experiments, due to the nature of the MD simulation (fixed atomic partial charges) the charge transfer between DNA and CNT upon hybridization was not taken into account. In another study using replica exchange MD (REMD), Roxbury *et al.* determined the charge density to be 4.5-6.0 $e/nm$ for a hybrid in which the same (6,5) CNT was wrapped by an ssDNA with the sequence being $(TAT)_4$;[18] the reported range, instead of a single value, was due to different number of strands (1 to 4) simulated in their work .

While the above studies focused on determining the charge of the hybrid, others attempted to understand the mechanism of separation by examining the electric field of the hybrid. The observation that ssDNA-CNT hybrids with different CNT chiralities elute at different time implies that the strength of electrostatic interaction between the hybrid and the IEC column depends on the electronic response of the CNT. Motivated by this, several studies have been performed to explore the electric field of a charged entity near an electronically responsive media.[15,19–23] The electrostatic potential of a line of charges in an electrolyte solution near a metallic, dielectric or semiconducting half space was analytically solved using PB theory by Tang *et al.*,[19] which was shown to strongly depend on the nature of the half-space. Malysheva *et al.* presented an analytical solution for the electrostatic potential of a more complicated system which contained a charged wall (representing IEC) and a hybrid consisting of a charged polyelectrolyte (representing DNA) and an electronically responsive cylinder (representing CNT), both embedded in an electrolyte solution.[21] Using the electrostatic potential, they determined the binding force between the wall and the hybrid and showed that the presence of a grounded metallic cylinder reduced the magnitude of the electric field of the polyelectrolyte and resulted in a smaller binding force compared with

the polyelectrolyte hybridized with a neutral dielectric cylinder. More recently, Malysheva *et al.* employed the one-dimensional density of state of CNT[24] and the Debye-Hückel equation[25] to evaluate the electrostatic potential of the hybrid.[26] As an approximation, the DNA charges were smeared out onto a cylindrical surface with the same axis as the CNT. The metallic CNT was shown to possess larger induced charge compared with the semiconducting one which resulted in smaller magnitudes of total charge and electrostatic potential for the hybrid, consistent with their previous work. Using semi-empirical tight binding method, Rotkin and Snyder indicated that DNA charges induced an electron density on CNT surface and changed its electronic structure.[27] They showed that the electrostatic potential of an ssDNA on a (7,0) CNT surface was approximately half of the corresponding value if no CNT was involved.[28] Although the above studies were useful in qualitatively describing the electric field of the hybrid, they were based on several assumptions including simplified geometries to represent DNA and CNT. Furthermore, DNA sequence which was shown to be very important in the experiments was not taken into account in those studies.

At a much smaller scale, a series of quantum mechanics (QM) simulations have been also performed to model the DNA-CNT hybrids; however, the focus of those studies was mainly on the structure and energy of binding.[29–54] To the best of our knowledge, there has not been any work at the atomistic level (using QM or even classical molecular mechanics (MM) simulations) to study the electrostatics of the DNA-CNT hybrids due to the complexity of the problem. Classical MM approaches can be used to simulate relatively large DNA-CNT hybrids in solution, however they can neither accurately describe the CNT's electronic structure nor distinguish the CNTs according to their chiralities. To capture CNT's electronic properties as well as the charge transfer upon hybridization, using QM approaches to model DNA and CNT is inevitable; however, the usability of atomistic QM methods is limited by the size of the system.

As the first attempt to study electrostatics of the ssDNA-CNT hybrid at the atomistic level, in this work, we perform a simulation to determine the electrostatic potential of a DNA nucleotide hybridized with a CNT in presence of explicit water and ions. The nucleotide, as a building block of DNA, is expected to capture the charged nature of the DNA backbone, while keeping the amount

of computation manageable. A combined QM:MM approach was employed in order to take into account the electron redistribution upon nucleotide-CNT binding, as well as to include the effect of electrolyte solution. In Section 2, computational details are described. Results of the electrostatic potential and charge transfer calculations are presented in Section 3 and conclusions are given Section 4.

## 2 Simulation details

In total, eight systems were simulated in this work, using a QM:MM scheme developed in our previous work.[55] Readers can refer to Ref.[55] for details of the method. Four DNA nucleoside monophosphates (NMPs) were considered in this study: adenosine 5'-monophosphates (AMP), cytidine 5'-monophosphates (CMP), guanosine 5'-monophosphates (GMP), and thymidine 5'-monophosphates (TMP). The corresponding molecular structure of the NMPs is shown in Fig. 1(a)-(d). Each NMP carries a charge of -2 due to the presence of two negatively charged oxygen atoms in its phosphate group.[56–58] Two CNTs (Fig. 1(e) and 1(f)) with different chiralities, (7,0) and (4,4), but similar length (respectively 15.6 and 14.8 Å) and diameter (respectively 5.48 and 5.42 Å) were considered to interact with the NMPs. Since applying periodic boundary condition (PBC) was not possible due to the limitations of the QM:MM approach,[59] hydrogen atoms were used to saturate the dangling bonds at the CNT ends. For each system, using Gromacs,[60] a water box with dimensions of $3 \times 2.4 \times 2\ nm^3$ was created and the NMP-CNT hybrid was solvated inside the box. In addition, we added two $Na^+$ cations, by random placement, to the solution so that each simulation system is charge neutral.

The simulations were performed using ONIOM approach in Gaussian 09.[59] A QM region and an MM region were defined for each simulated systems. The QM region contains all atoms in the CNT and NMP while the rest of the atoms i.e., all water molecules and the two cations were considered in the MM region. To perform the ONIOM simulation, we chose density functional theory (DFT) along with M06-2X functional for the QM calculations and Amber force-field for the

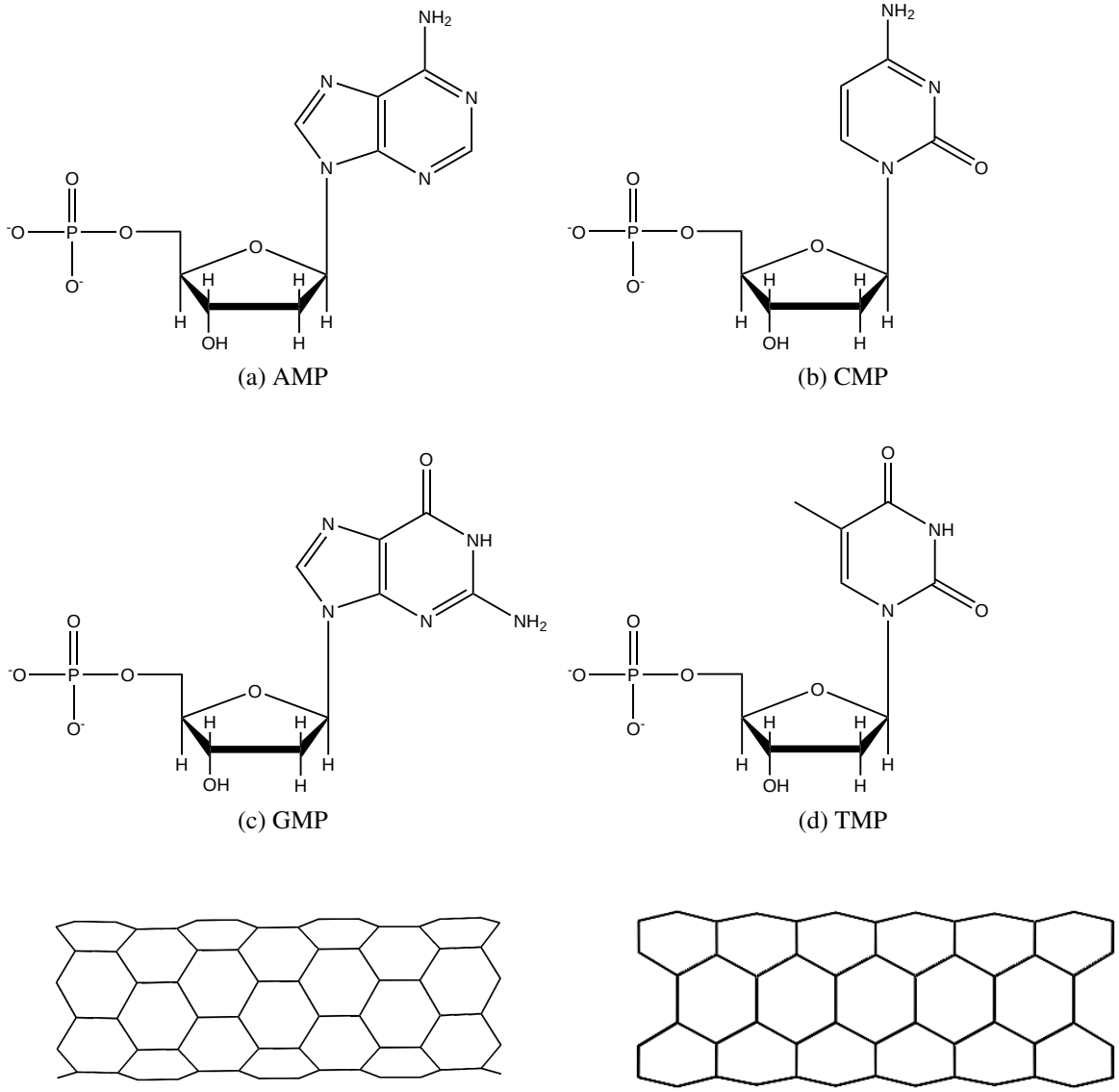


(a) AMP (b) CMP

(c) GMP (d) TMP

(e) (7,0) CNT (f) (4,4) CNT

Figure 1: Molecular structures of NMPs and CNTs simulated in this work.

MM calculations. Each system was optimized according to the following procedures, as described in detail in Ref.:[55]

1. Individual NMP and CNT were optimized in vacuum using DFT with M06-2X functional and the basis set of 6-31G(d). Partial atomic charges (based of restrained electrostatic potential (Resp)[61] method) were calculated for the individually optimized NMP and CNT using Amber-Tools.[62]

2. The simulation system was constructed using the relaxed NMP and CNT as well as water and $Na^+$ cations. It was then subjected to an MM optimization, using the partial charges obtained from step 1.

3. An ONIOM optimization was performed for the relaxed structures obtained from step 2.

4. Electrostatic potential and charge transfer were evaluated for the optimized hybrids obtained from step 3. The details of the calculations are explained below.

Electrostatic potential, $\phi$, was obtained directly from the QM:MM simulations and evaluated at three dimensional grid points in the space surrounding the NMP-CNT hybrid. As pointed out in the introduction, ssDNA-CNT hybrids with different CNT chiralities appear to have different strengths of attraction to the IEC, that is, they likely have different electrostatic potential at the location of the IEC. Therefore, we are interested in the electrostatic potential of the hybrid in its encompassing cylindrical region and will use the cylindrical coordinate shown in Fig. 2 (optimized AMP-(4,4) CNT hybrid as an example) to analyze the results. In this coordinate, the CNT axis is set to be the $Z$-axis. The origin of the coordinate system is defined as the projection of the NMP's center of mass (COM) onto the $Z$-axis. $Y$-axis is set to be the axis passing through the NMP's COM and the origin, and $X$-axis is perpendicular to both $Y$ and $Z$ axes (See Fig. 2(b)). The polar coordinates, $r$ and $\theta$, are defined in the $X-Y$ plane where $r$ is the radial distance from the origin and $\theta$ is the counterclockwise angle measured from the $X$-axis. In addition, it was found that the largest separation distance between all NMP atoms and the CNT axis was $\sim$10 Å. Since in the IEC experiment, the surface of the IEC column is expected be located near the hybrid, the range of the radial coordinate, $r$, was chosen to be between 12 Å and 15 Å throughout the paper. The $Z$

coordinate was varied from -20 Å to 20 Å which is large enough to cover the length of the CNT. Finally, $\theta$ is varied from 0° to 360°.

For the charge transfer, we first employed the Resp approach to calculate the atomic partial charges on the NMP and CNT atoms, as well as on the two $Na^+$ ions. The Resp scheme was chosen because it generates atomic partial charges at atom centers to reproduce the electrostatic potential in the space, hence is consistent with the electrostatic potential calculations in this work. Water molecules were removed from the molecular model in the charge transfer calculation due to computational limitations.[62] Instead, we used the conductor-like polarizable continuum model (CPCM)[63] which is the most commonly employed implicit model for the solution. Since the initial net charge in each NMP is -2, the charge transfer was determined as the $\delta = q - (-2)$, where $q$ is the final net charge of the NMP. Positive $\delta$ corresponds to electron transfer from NMP to CNT.

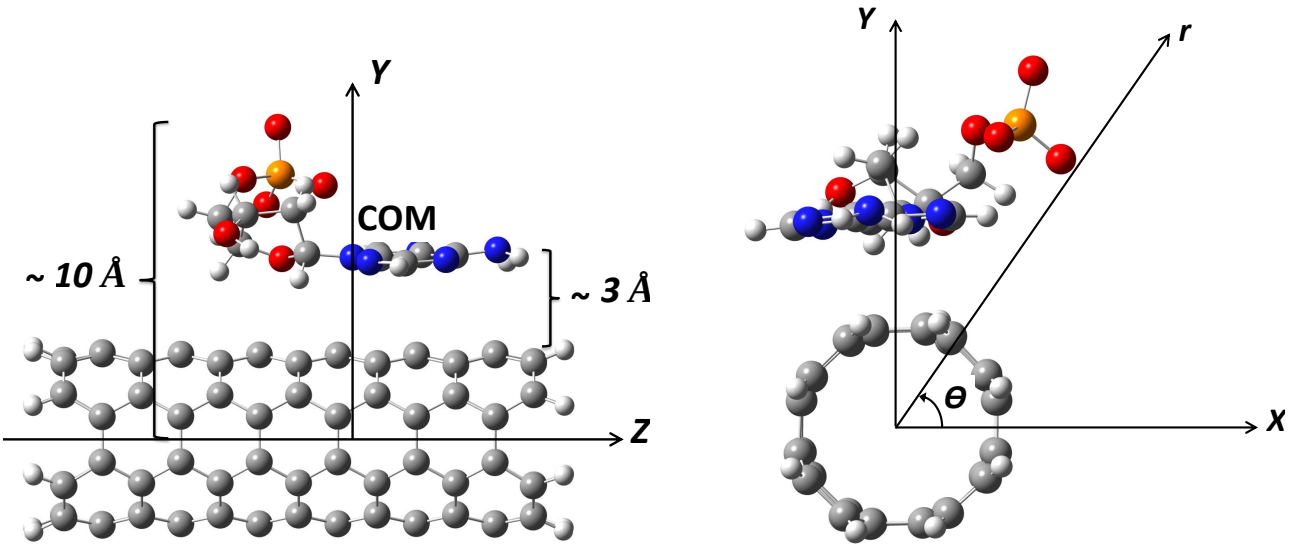


(a) (b)

Figure 2: The representation of the cylindrical coordinate (using AMP-(4,4) CNT hybrid): a. Side view; b. Front view. COM marks the center of mass of the AMP.

# 3 Results and discussion

## 3.1 Electrostatic Potential

The final optimized structure for the AMP-(4,4) CNT hybrid is shown in Fig. 2 where the water and ions are not shown for the purpose of clarity. Similar final configurations were obtained for the rest of NMP-CNT hybrids. More specifically, nucleobases possessed a parallel orientation with respect to the CNT surface with a separation distance of $\sim$3 Å while the phosphate group tends to expose itself to the solution phase. Distributions of the electrostatic potential for the AMP-(4,4) CNT hybrid at the radial distance of 15 Å is shown in Fig. 3 (The corresponding distributions for all the eight systems are compared in Fig. S1 of the Supporting Information). In these plots, the electrostatic potential is depicted versus $Z$ (CNT axis) and $\theta$ axes, and its magnitude is highlighted by the color. While all values are negative due to the negative charges on the NMPs, the blue and red regions respectively correspond to the most and least negative values.

For all systems, a valley-shaped distribution for the electrostatic potential, $\phi$, is obtained. The minimum value of $\phi$ present in each system (located in the valley and colored blue), $\phi_{min}$, corresponds to the lowest electrostatic potential at the radial distance of $r =$15 Å. The $\theta$ and $Z$ coordinates at $\phi_{min}$ are about 90° and 0, respectively. In other words, at $r =$15 Å, $\phi_{min} = \phi(\theta =\sim 90^{\circ}, Z =\sim 0)$, which is a location on this cylindrical surface relatively close to the phosphate group of NMPs (see Fig. 2). This is expected due to the concentration of the negative charge in the phosphate group. The location of $\phi_{min}$ is important because if an external charged entity (such as the IEC column) is present, it will have the strongest interaction with the hybrid where the minimum electrostatic potential is found. The magnitude of $\phi_{min}$ is also of significance since it measures the strength of interaction, and more generally is an indication for the molecular reactivity in biological systems.[64–66]

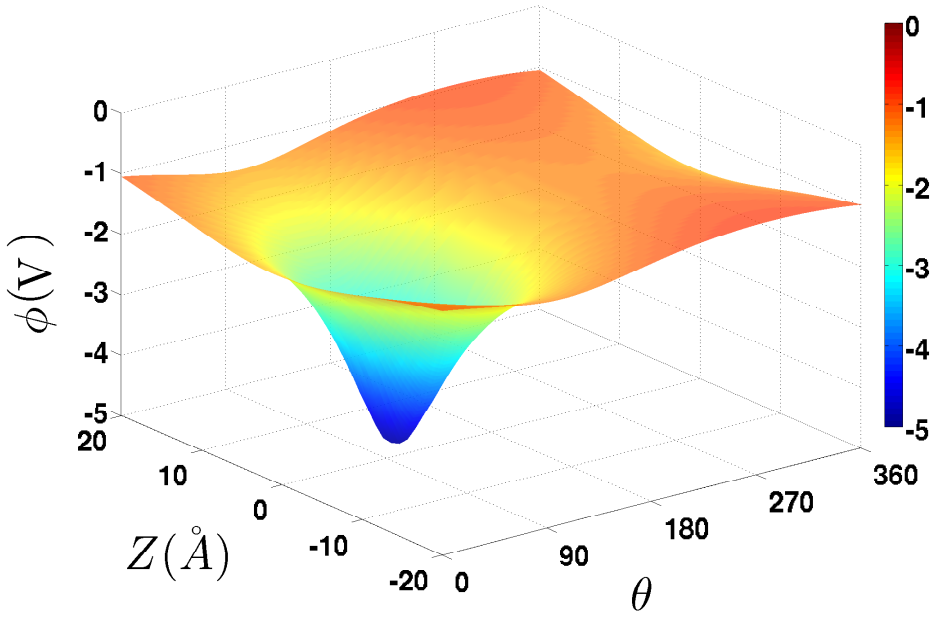


(a) AMP-(4,4)CNT

Figure 3: Distribution of the electrostatic potential ($\phi$) for AMP-(4,4) CNT hybrid as a function of $Z$ and $\theta$. The radial distance is fixed at $r$=15 Å.

Similar distributions of $\phi$ for smaller radial distances, i.e., 12 Å $< r <$15 Å , was also obtained. More specifically, at a given $r$ a minimum was found in the vicinity of the phosphate group in all eight systems. To examine $\phi_{min}$ in detail, we obtain $\phi_{min}$ at each radial distance and plot it as a function of $r$ in Fig. 4. Different curves in Fig. 4 correspond to different simulated systems, and they all show a similar trend of $\phi_{min}$ versus $r$. Specifically, each curve starts with the most negative value of $\phi_{min}$ at $r =$12 Å , gradually increases with $r$, and shows the trend of converging to zero as $r$ tends to infinity. More negative $\phi_{min}$ is obtained for smaller values of $r$ because the potential is evaluated at points closer to the negatively charged zone of the NMP. The minimum value of the electrostatic potential on the molecular surface of the isolated nucleobases in vacuum was determined by Pullman *et al.* to be -2.25, -1.34, -1.99, and -1.23 V, respectively for guanine, adenine, cytosine, and thymine.[65] For the nucleotides, more negative values for the minimum electrostatic potential was reported due to the inclusion of the negatively charged phosphate group.[66] Pullman

and Pullman studied the electrostatic potential of dimethylphosphate (with a net charge of -1) as a model to represent the phosphate group in DNA. The minimum electrostatic potential was reported to be -8.67 V at a distance of 1.05 Å from the anionic oxygen bound to the phosphors in a plane defined by the phosphorous and two anionic oxygen atoms.[64] Considering all NMP-CNT systems, the range of $\phi_{min}$ is [-10.30,-4.28] V at $r$ =12 Å and [-4.90, -2.95] V at $r$ =15 Å, which is similar in magnitude to the $\phi_{min}$ of dimethylphosphate. More direct comparison cannot be made between the electrostatic potential of the NMP-CNT hybrids and that of the dimethylphosphate for several reasons. Firstly, the dimethylphosphate had a net charge of -1 while each of the NMPs we simulated has a net charge of -2. Secondly, the dimethylphosphate was isolated while our NMPs are under the influence of the CNT. In addition, the dimethylphosphate was located in vacuum while our hybrids were solvated. The highly polar solvent (water) and the ions can create a screening effect for the electrostatic field. Also, the electrostatic potential in Ref.[64] was evaluated at a distance of 1.05 Å from the anionic oxygen, while the electrostatic potential in our systems was evaluated at larger distances from the two anionic oxygen atoms.

Despite the qualitative similarity in the dependence of $\phi_{min}$ on $r$, quantitatively, $\phi_{min}$ is quite different for different NMP-CNT hybrids. At any given $r$, the absolute value of $\phi_{min}$ follows the order, from small to large, of TMP-(7,0) CNT, AMP-(7,0) CNT, GMP-(7,0) CNT, CMP-(4,4) CNT, TMP-(4,4) CNT, CMP-(7,0) CNT, GMP-(4,4) CNT, and AMP-(4,4) CNT. Clearly, the electrostatic potential of the hybrids strongly depends on the chirality of the CNT as well as the type of nucleobase in the NMP.

First let us consider the effect of CNT. Except for CMP, NMP-(4,4) CNT hybrids generates stronger electrostatic potential compared with the NMP-(7,0) CNT hybrids. For example, $\phi_{min}$ at $r = 12$ is -4.39, -7.10, -4.79, and -4.28 V, respectively for AMP, CMP, GMP, and TMP adsorbed to the (7,0) CNT. For the hybrids formed by NMPs and the (4,4) CNT, $\phi_{min}$($r$=12 Å) is -10.30, -5.41, -8.93, and -6.13 V, respectively for AMP, CMP, GMP, and TMP. Although the two CNTs possess similar length and diameter, their different chiralities lead to very different electrostatic potential when they interact with the NMPs. To the best of our knowledge, there is no work at

atomistic level to study the electrostatic potential of the hybrid. In the continuum-based study of Malysheva *et al.*, it was shown that an ssDNA-metallic CNT hybrid generates smaller magnitudes of electrostatic potential compared with an ssDNA-semiconducting CNT hybrid[26] which would predict easier elution of ssDNA-metallic CNT hybrids observed in early IEC experiments.[1,11] The stronger electrostatic potential we found from our simulations for (4,4) CNT, which is seemingly contradicting to the earlier studies,[1,11] may be first due to the fact that the CNTs in this study have finite lengths (caused by the incapability of including PBC within the QM:MM scheme[59]) and hence may not truly reflect the metallic/semiconducting properties of long CNTs. To explore why NMP-(4,4) CNT hybrids generates stronger electrostatic potential, we calculated the separation distance between the NMP atoms and the CNT surface. It was found that except for CMP, the phosphate group in the NMP-(7,0) CNT hybrids is located closer to the CNT compared with that in the NMP-(4,4) CNT hybrids.[55] In other words, the (7,0) CNT binds more tightly with the NMPs compared with the (4,4) CNT (with the exception of CMP), which is also confirmed by examining the atomic separations and binding energy (see Ref.[55] for detailed results of the binding energy calculations as well as binding structures). The stronger binding can lead to stronger charge transfer (as will be demonstrated in the next section) from the NMP to the CNT, and the wider distribution of charges in space (as compared to concentrated charge at the phosphate group) can cause reduction in the magnitude of electrostatic potential. In other words, the electrostatic field of the hybrid may not be only influenced by the electronic property of the CNT, but also by their binding strength and structure. It should be mentioned that some experiments revealed that semiconducting CNTs were more weakly adsorbed to the IEC and eluted earlier compared with metallic CNTs[14] which implied the complexity of the DNA-CNT interactions.

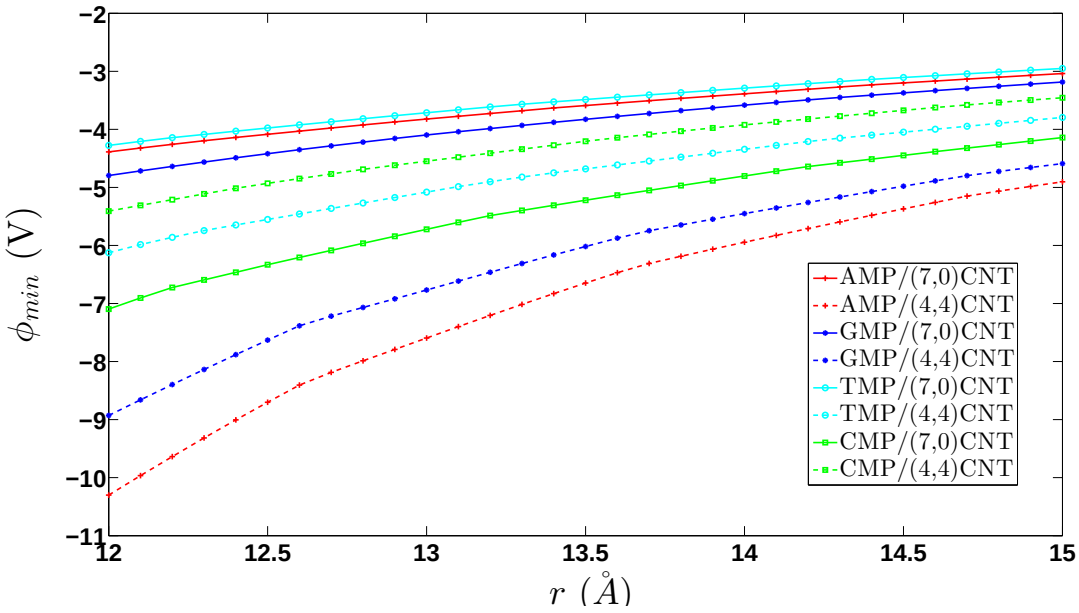


Figure 4: Minimum of the electrostatic potential $\phi_{min}(r)$ for different simulated systems. At each radial distance $r$, the electrostatic potential is calculated as a function of $Z$ and $\theta$ (e.g. see Figure 3), and the minimum value is reported as $\phi_{min}(r)$.

In addition to the influence from the CNTs, the electrostatic potential of the hybrid is also affected by the type of nucleobase in the NMP. When the absolute value of $\phi_{min}$ is ranked according to the NMP, the order is CMP>GMP∼AMP∼TMP for the NMP-(7,0) CNT hybrids and AMP>GMP>TMP>CMP for the NMP-(4,4) CNT hybrids. The different orders of $\phi_{min}$ for the two CNTs suggests that the types of CNT and NMP have coupled roles in determining the electrostatic potential of the hybrids. To further explore this, we defined the difference in minimum electrostatic potential, $\Delta\phi_{min}$, presented in equation 1.

$$\Delta\phi_{min}(r) = |\phi_{min}^{(7,0)\ CNT}(r) - \phi_{min}^{(4,4)\ CNT}(r)| \tag{1}$$

For each NMP, $\Delta\phi_{min}$ was evaluated at each $r$ in the range of 12 Å to 15 Å and is shown in Fig. 5. According to the figure, $\Delta\phi_{min}$ decays as $r$ becomes larger and is expected to converge to zero as $r$ tends to infinity, since $\phi_{min}$ approaches zero in all systems (see Fig. 4). Interestingly, for all values

of $r$, $\Delta\phi_{min}$ for AMP and GMP are considerably larger than that for CMP and TMP. For instance, for almost all $r$, $\Delta\phi_{min}$ of GMP is more than twice that of TMP and CMP, and $\Delta\phi_{min}$ from AMP is more than three times larger. This implies that the type of nucleobase in the NMPs remarkably influence the electrostatic potential of the hybrid, although all NMPs carry the same amount of negative charge and have the sugar ring and phosphate group in common. Quantitatively, $\Delta\phi_{min}$ is a measure on the easiness of distinguishing the two types of CNTs. The significantly larger $\Delta\phi_{min}$ caused by AMP and GMP suggests that the two CNTs can be more easily differentiated and potentially separated with these two types of NMPs. In the separation of CNT using ssDNA in the IEC, it has been shown that the separation is very sensitive to the DNA sequence.[11] Although the simulations here do not involve DNA polymer, our results for $\Delta\phi_{min}$ can provide some clues on why the separation depends on the type and sequence of nucleotides.

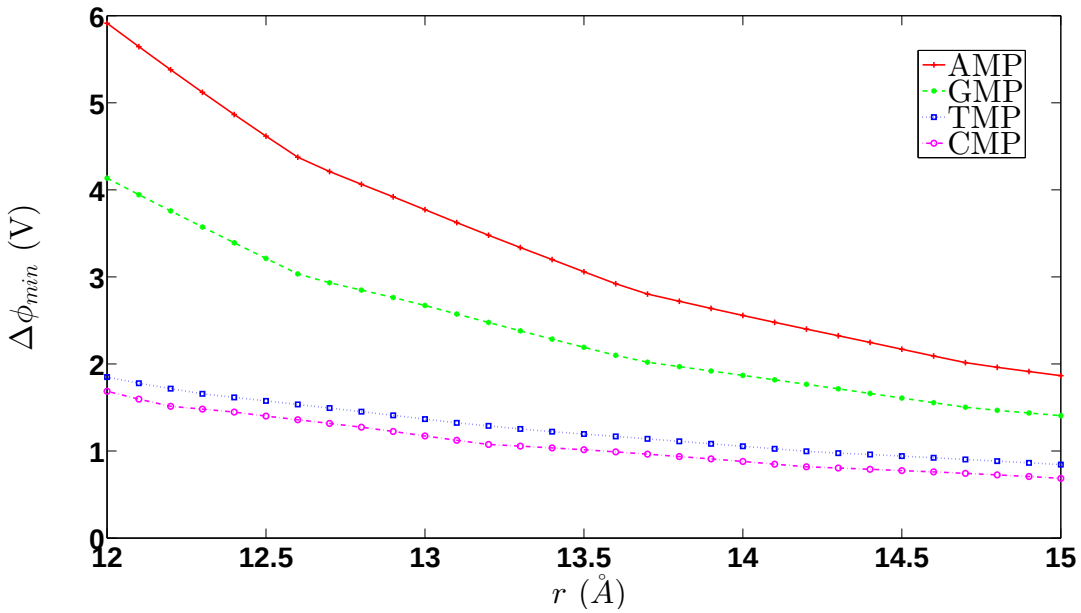


Figure 5: Difference in the minimum electrostatic potential between NMP-(4,4) CNT hybrid and NMP-(7,0) CNT hybrid. Each minimum electrostatic potential is evaluated at a given distance $r$ from the CNT axis.

## 3.2 Charge Transfer

Final partial atomic charges of the nucleotides and CNTs for all eight systems are presented in the Supporting Information (Figure S2 and Figure S3). The charge transfer, $\delta$, between each NMP and CNT was calculated and is presented in Table 1. For two of the hybrids, AMP-(4,4) CNT and GMP-(4,4) CNT, the adsorption took place without noticeable charge transfer. In the other six hybrids, a partial electronic charge was transferred from the NMP to the CNT and hence the CNT became negatively charged upon the hybridization. In these six systems, $\delta$ ranges from 0.08 to 0.65 *e*: it is similar (around 0.1 *e*) for the CMP-(4,4) CNT, TMP-(4,4) CNT, AMP-(7,0) CNT, and CMP-(7,0) CNT; while for GMP and TMP adsorbed on the (4,4) CNT, $\delta$ is considerably large (around 0.6 *e*).

Unlike the lack of reports on the electrostatic potential in the literature, the charge transfer between the nucleotide/nucleobase and CNT has been reported in some of the past studies, all based on using QM approaches. For instance, Shukla *et al.* determined the charge transfer to be 0.02-0.04 *e* from DNA nucleobases to a (7,0) CNT using DFT (M05-2X functional) and Mulliken approach.[49] Using DFT(LDA) and Bader analysis, Gowtham *et al.* showed that a small amount of electric charge, 0.05 and 0.08 *e*, was transferred respectively from adenine and guanine to a (5,0) CNT.[31] Das *et al.* studied the adsorption of DNA nucleobases onto a (5,5) CNT using Mulliken population and showed that the charges were only redistributed among the atoms without any net charge transfer between nucleobases and the CNT.[67] Clearly, the charge transfer between DNA nucleobases and CNT are essentially negligible, due to the absence of the charged phosphate group. Enyashin *et al.*, using self consistent charge density-functional based tight-binding method (SCC-DFTB), reported 0.2-0.4 *e* charge transfer from a PolyC-DNA to CNTs with the chiralities of (8,2) and (7,4), and less than 0.05 *e* for CNTs with the chiraliteis of (5,5), (7,3), (8,0), and (10,0).[47]Considering that the hybrids involved polymer DNA, the charge transfer is still insignificant. This is because although the phosphate groups were included, they were not deprotonated and hence the DNAs simulated were neutral. The only work where the charge transfer was found to be significant is by Wang and Ceulemans, who evaluated the charge transfer for two connected

AMPs adsorbed on CNTs using Mulliken approach.[35] The simulations were also performed in vacuum and the two connected AMPs were charge neutral. Charge transfer of 0.85 and 0.56 *e* was found, respectively for (7,0) and (4,4) CNTs, but in contrary to all other studies, the direction of the transfer was from the CNT to the AMPs, which is not yet understood.

It should be pointed out that the charge transfer calculations are quite sensitive to the choice of the QM approach as well as the charge calculation scheme. It has been shown that very different results for the charge transfer in the biological systems may be obtained based on different selections of the QM and charge calculation methods.[68] It is well known that the Mulliken charge scheme, although most widely used due to its simplicity, poorly describes the molecular properties especially the electrostatic potential.[69] On the other hand, Resp approach, employed in our study, is known to accurately reproduce the electrostatic potential of the molecular systems. Our finding that hybrids with (7,0) CNT generally have larger charge transfer compared with the (4,4) CNT is consistent with the electrostatic potential results discussed in Section 3.1, and both can be explained in terms of the tightness of the binding. As mentioned earlier, the NMPs are more tightly bound to the (7,0) CNT compared with the (4,4) CNT,[55] which may facilitate the charge transfer between the two entities, and this is evidence by the data shown in Table 1. The correlation between binding strength and charge transfer was also reported by Lu *et al.*, who showed that the physisorption of naphthalene, anthracene, and tetracyanoquinodimethane (TCNQ) on a (6,6) CNT was in general stronger compared with those on a (10,0) CNT, which was accompanied by higher charge transfer to the (6,6) CNT.[70] On the other hand, for the NMPs adsorbed onto the same CNT, the order of the charge transfer is more complex, and cannot be explained by the tightness of binding alone. For example, for the (4,4) CNT, the energy of binding for the four NMPs was found to follow the order of GMP>TMP>CMP>AMP.[55] The corresponding order for the charge transfer is CMP>TMP>GMP∼AMP. For the (7,0) CNT, the order of the energy of binding was shown to be TMP>AMP>GMP>CMP[55] while the order for the charge transfer is GMP>TMP>CMP>AMP. One possible explanation might be the position and orientation of the NMPs relative to the CNT. It is well known that the potential energy surface (PES) for nucleobase-CNT hybrids is shallow with

many possible local minima,[32,33,54] which is likely also true for the NMP-CNT hybrids. These local minima can correspond to the similar binding energy but different configurations of the NMPs relative to the CNT, which can result in different charge transfers. Leenaerts *et al.* evaluated the energy of binding and charge transfer upon the adsorption of $H_2O$, $NH_3$, CO, $NO_2$, and NO on graphene. They showed that different relative configurations (adsorption site and orientation) of the adsorbed molecules may result in the same energy of binding, but completely different values of the charge transfer.[71]

**Table 1: Charge transfer ($e$) between NMPs and CNTs**

| | AMP | CMP | GMP | TMP |
|---|---|---|---|---|
| (4,4) CNT | $\sim 0$ | 0.10 | $\sim 0$ | 0.08 |
| (7,0) CNT | 0.12 | 0.15 | 0.65 | 0.54 |

Compared with past works in literature, the present work adopted an atomistic QM:MM approach and evaluated the electrostatic potential generated by the NMP-CNT hybrid for the first time. An electrolytic environment was introduced, which has two consequences: the charged NMPs as well as the polar medium around the hybrids. This was never done in previous QM studies, but is essential and better mimics the conditions in most experiments involving these hybrids (e.g., the CNT separation experiments using IEC). The presence of solution is important to the properties of the hybrids including binding structure and strength, as well as electrostatic potential. For instance, the contribution of water release to the binding energy between NMPs and CNTs has been shown to be considerable.[55] The polarization of the CNT by the NMPs and the solution was taken into account so as to produce accurate electron density, which is not possible with classical MM or continuum approaches. Therefore, our work is an important step toward more comprehensive modeling of the DNA-CNT hybrids.

Despite these merits, several limitations, caused by the current limitations in computational capacity and methodology, should be addressed. First, applying PBC or simulating a relatively long CNT is essential in order to precisely resemble the electronic properties of the bulk CNT. Second,

a larger number of nucleotides should be included in order to resemble a long DNA interacting with the CNT. Presence of a longer piece of DNA may introduce other influential factors in its interactions with CNTs. For instance, it has been shown that the wrapping angle which is affected by the length of the ssDNA plays an important role in the properties of the hybrid.[15] In addition, only two $Na^+$ cations were considered in this work to just neutralize the system. Different type and concentrations of salt may affect the properties of the hybrids, as it has been shown that the number of ions affects the energy of binding between NMPs and a (6,0) CNT.[56] The effect on the electrostatic potential and charge transfer requires a series of separate simulations with different salt types and concentrations. Last, the explicit water molecules were replaced by a continuum model in the charge transfer calculations which may reduce the accuracy of the partial atomic charge calculation. It is important to develop computationally affordable QM:MM methods to reduce the aforementioned limitations in order to more precisely study the properties of the ssDNA-CNT hybrids.

# 4 Conclusions

Using a QM:MM method, the electrostatic potential and charge transfer was evaluated for the hybrids formed by DNA nucleotides and CNTs in aqueous solution. It is the first model that included QM description of the CNT and nucleotide under the influence of the electrolytic environment, and explicitly calculated electrostatic potential from atomic simulations. It is shown that the electrostatic potential of the hybrid in its vicinity strongly depends on the type of nucleotide and the chirality of the CNT. At the same distance from the CNT axis, the NMP-(4,4) CNT hybrids were found to generate stronger electrostatic potential compared with the NMP-(7,0) CNT hybrids. Atomic charge calculations also showed stronger charge transfer from the NMP to the CNT in the case of (7,0) CNT. Compared with our previous findings where NMPs were shown to generally bind tighter to the (7,0) CNT compared with the (4,4) CNT, these results suggest the electrostatics of the DNA-CNT hybrids may be influenced by the tightness of the binding. AMP

and GMP were found to produce larger difference in electrostatic potential when they bind to the two types of tubes, indicating their better capability of distinguishing the two CNTs.

## Acknowledgement

This work was supported by the Natural Science and Engineering Research Council (NSERC) of Canada through the Canada Research Chair program and Discovery Grant, and by Alberta Innovates Technology Futures. Chehel Amirani acknowledges the support from Sadler Graduate Scholarship in Mechanical Engineering at the University of Alberta. Authors would like to thank WestGrid and Compute/Calcul Canada for providing computing resources.

## References

(1) Zheng, M.; Jagota, A.; Semke, E. D.; Diner, B. A.; Mclean, R. S.; Lustig, S. R.; Richardson, R. E.; Tassi, N. G. DNA-assisted dispersion and separation of carbon nanotubes. *Nat Mater* **2003**, *2*, 338–342.

(2) Dwyer, C.; Guthold, M.; Falvo, M.; Washburn, S.; Superfine, R.; Erie, D. DNA-functionalized single-walled carbon nanotubes. *Nanotechnology* **2002**, *13*, 601.

(3) Shin, S. R.; Lee, C. K.; So, I. S.; Jeon, J. H.; Kang, T. M.; Kee, C. W.; Kim, S. I.; Spinks, G. M.; Wallace, G. G.; Kim, S. J. DNA-Wrapped Single-Walled Carbon Nanotube Hybrid Fibers for supercapacitors and Artificial Muscles. *Advanced Materials* **2008**, *20*, 466–470.

(4) Arnett, C. M.; Marsh, C. P.; Welch, C. R.; Strano, M. S.; Han, J.-H.; Gray, J. H.; Carlson, T. A. Enzyme-Mediated Assimilation of DNA-Functionalized Single-Walled Carbon Nanotubes. *Langmuir* **2010**, *26*, 613–617, PMID: 19957946.

(5) Yang, R.; Tang, Z.; Yan, J.; Kang, H.; Kim, Y.; Zhu, Z.; Tan, W. Noncovalent Assembly

of Carbon Nanotubes and Single-Stranded DNA: An Effective Sensing Platform for Probing Biomolecular Interactions. *Analytical Chemistry* **2008**, *80*, 7408–7413, PMID: 18771233.

(6) Wang, H.; Muren, N. B.; Ordinario, D.; Gorodetsky, A. A.; Barton, J. K.; Nuckolls, C. Transducing methyltransferase activity into electrical signals in a carbon nanotube-DNA device. *Chem. Sci.* **2012**, *3*, 62–65.

(7) Kilina, S.; Yarotski, D. A.; Talin, A. A.; Tretiak, S.; Taylor, A. J.; Balatsky, A. V. Unveiling Stability Criteria of DNA-Carbon Nanotubes Constructs by Scanning Tunneling Microscopy and Computational Modeling. *Journal of Drug Delivery* **2011**, *2011*.

(8) Bratcher, M.; Gersten, B.; Ji, H.; Mays, J. Study in the Dispersion of Carbon Nanotubes. Symposium Z Making Functional Materials with Nanotubes. 2001.

(9) Tchoul, M. N.; Ford, W. T.; Lolli, G.; Resasco, D. E.; Arepalli, S. Effect of Mild Nitric Acid Oxidation on Dispersability, Size, and Structure of Single-Walled Carbon Nanotubes. *Chemistry of Materials* **2007**, *19*, 5765–5772.

(10) Rinzler, A.; Liu, J.; Dai, H.; Nikolaev, P.; Huffman, C.; Rodriguez-Macias, F.; Boul, P.; Lu, A.; Heymann, D.; Colbert, D.; Lee, R.; Fischer, J.; Rao, A.; Eklund, P.; Smalley, R. Large-scale purification of single-wall carbon nanotubes: process, product, and characterization. *Applied Physics A* **1998**, *67*, 29–37.

(11) Zheng, M.; Jagota, A.; Strano, M. S.; Santos, A. P.; Barone, P.; Chou, S. G.; Diner, B. A.; Dresselhaus, M. S.; Mclean, R. S.; Onoa, G. B.; Samsonidze, G. G.; Semke, E. D.; Usrey, M.; Walls, D. J. Structure-Based Carbon Nanotube Sorting by Sequence-Dependent DNA Assembly. *Science* **2003**, *302*, 1545–1548.

(12) Tu, X.; Zheng, M. A DNA-based approach to the carbon nanotube sorting problem. *Nano Research* **2008**, *1*, 185–194.

(13) Zheng, M.; Semke, E. D. Enrichment of Single Chirality Carbon Nanotubes. *Journal of the American Chemical Society* **2007**, *129*, 6084–6085, PMID: 17458969.

(14) Tu, X.; Manohar, S.; Jagota, A.; Zheng, M. DNA sequence motifs for structure-specific recognition and separation of carbon nanotubes. *Nat Mater* **2009**, *460*, 250–253.

(15) Lustig, S. R.; Jagota, A.; Khripin, C.; Zheng, M. Theory of Structure-Based Carbon Nanotube Separations by Ion-Exchange Chromatography of DNA/CNT Hybrids. *The Journal of Physical Chemistry B* **2005**, *109*, 2559–2566.

(16) Khripin, C. Y.; Manohar, S.; Zheng, M.; Jagota, A. Measurement of Electrostatic Properties of DNA-Carbon Nanotube Hybrids by Capillary Electrophoresis. *The Journal of Physical Chemistry C* **2009**, *113*, 13616–13621.

(17) Zur, S. O. Theorie der Elektrolytischen Doppelschicht. *Electrochem* **1924**, *30*, 508–16.

(18) Roxbury, D.; Jagota, A.; Mittal, J. Structural Characteristics of Oligomeric DNA Strands Adsorbed onto Single-Walled Carbon Nanotubes. *The Journal of Physical Chemistry B* **2013**, *117*, 132–140.

(19) Tang, T.; Hui, C.-Y.; Jagota, A. Line of charges in electrolyte solution near a half-space: II. Electric field of a single charge. *Journal of Colloid and Interface Science* **2006**, *299*, 572 – 579.

(20) Malysheva, O.; Tang, T.; Schiavone, P. Adhesion between a charged particle in an electrolyte solution and a charged substrate: Electrostatic and van der Waals interactions. *Journal of Colloid and Interface Science* **2008**, *327*, 251 – 260.

(21) Malysheva, O.; Tang, T.; Schiavone, P. Binding Force Between a Charged Wall and a Complex Formed by a Polyelectrolyte and an Electronically Responsive Cylinder. *The Journal of Adhesion* **2011**, *87*, 251–271.

(22) Zheng, M.; Eom, K.; Ke, C. Calculations of the resonant response of carbon nanotubes to binding of DNA. *Journal of Physics D: Applied Physics* **2009**, *42*, 145408.

(23) Sun, C.; Tang, T. Structure of a polyelectrolyte around an electronically responsive cylinder. *Journal of Colloid and Interface Science* **2009**, *338*, 276 – 283.

(24) Mintmire, J. W.; White, C. T. Universal Density of States for Carbon Nanotubes. *Phys. Rev. Lett.* **1998**, *81*, 2506–2509.

(25) Russel, W.; Saville, D.; Schowalter, W. *Colloidal Dispersions*; Cambridge Monographs on Mechanics; Cambridge University Press, 1992.

(26) Malysheva, O.; Tang, T.; Schiavone, P. A model for carbon nanotubeDNA hybrid using one-dimensional density of states. *Journal of Colloid and Interface Science* **2012**, *380*, 25 – 33.

(27) Rotkin, S. V.; Snyder, S. E. *Carbon Nanotubes and Related Structures*; Wiley-VCH Verlag GmbH & Co. KGaA, 2010; pp 23–51.

(28) Snyder, S.; Rotkin, S. Polarization component of cohesion energy in single-wall carbon nanotube-DNA complexes. *JETP Letters* **2006**, *84*, 348–351.

(29) Chehel Amirani, M.; Tang, T. Binding of nucleobases with graphene and carbon nanotube: a review of computational studies. *Journal of Biomolecular Structure and Dynamics* **2014**, 1–31, PMID: 25118044.

(30) Gowtham, S.; Scheicher, R. H.; Ahuja, R.; Pandey, R.; Karna, S. P. Physisorption of nucleobases on graphene: Density-functional calculations. *Phys. Rev. B* **2007**, *76*, 033401.

(31) Gowtham, S.; Scheicher, R. H.; Pandey, R.; Karna, S. P.; Ahuja, R. First-principles study of physisorption of nucleic acid bases on small-diameter carbon nanotubes. *Nanotechnology* **2008**, *19*, 125701.

(32) Meng, S.; Maragakis, P.; Papaloukas, C.; Kaxiras, E. DNA Nucleoside Interaction and Identification with Carbon Nanotubes. *Nano Letters* **2007**, *7*, 45–50.

(33) Meng, S.; Wang, W. L.; Maragakis, P.; Kaxiras, E. Determination of DNA-Base Orientation on Carbon Nanotubes through Directional Optical Absorbance. *Nano Letters* **2007**, *7*, 2312–2316.

(34) Shtogun, Y. V.; Woods, L. M.; Dovbeshko, G. I. Adsorption of Adenine and Thymine and Their Radicals on Single-Wall Carbon Nanotubes. *The Journal of Physical Chemistry C* **2007**, *111*, 18174–18181.

(35) Wang, H.; Ceulemans, A. Physisorption of adenine DNA nucleosides on zigzag and armchair single-walled carbon nanotubes: A first-principles study. *Phys. Rev. B* **2009**, *79*, 195419.

(36) Wang, Y.; Bu, Y. Noncovalent Interactions between Cytosine and SWCNT. *The Journal of Physical Chemistry B* **2007**, *111*, 6520–6526, PMID: 17508735.

(37) Wang, Y. Theoretical Evidence for the Stronger Ability of Thymine to Disperse SWCNT than Cytosine and Adenine: Self-Stacking of DNA Bases vs Their Cross-Stacking with SWCNT. *The Journal of Physical Chemistry C* **2008**, *112*, 14297–14305.

(38) Ortmann, F.; Schmidt, W. G.; Bechstedt, F. Attracted by Long-Range Electron Correlation: Adenine on Graphite. *Phys. Rev. Lett.* **2005**, *95*, 186101.

(39) Berland, K.; Chakarova-Käck, S. D.; Cooper, V. R.; Langreth, D. C.; Schröder, E. A van der Waals density functional study of adenine on graphene: single-molecular adsorption and overlayer binding. *Journal of Physics: Condensed Matter* **2011**, *23*, 135001.

(40) Panigrahi, S.; Bhattacharya, A.; Banerjee, S.; Bhattacharyya, D. Interaction of Nucleobases with Wrinkled Graphene Surface: Dispersion Corrected DFT and AFM Studies. *The Journal of Physical Chemistry C* **2012**, *116*, 4374–4379.

(41) Chandra Shekar, S.; Swathi, R. S. Stability of Nucleobases and Base Pairs Adsorbed on Graphyne and Graphdiyne. *The Journal of Physical Chemistry C* **2014**, *118*, 4516–4528.

(42) Antony, J.; Grimme, S. Structures and interaction energies of stacked graphene-nucleobase complexes. *Phys. Chem. Chem. Phys.* **2008**, *10*, 2722–2729.

(43) Lee, J.-H.; Choi, Y.-K.; Kim, H.-J.; Scheicher, R. H.; Cho, J.-H. Physisorption of DNA Nucleobases on h-BN and Graphene: vdW-Corrected DFT Calculations. *The Journal of Physical Chemistry C* **2013**, *117*, 13435–13441.

(44) Le, D.; Kara, A.; Schröder, E.; Hyldgaard, P.; Rahman, T. S. Physisorption of nucleobases on graphene: a comparative van der Waals study. *Journal of Physics: Condensed Matter* **2012**, *24*, 424210.

(45) Cho, Y.; Min, S. K.; Yun, J.; Kim, W. Y.; Tkatchenko, A.; Kim, K. S. Noncovalent Interactions of DNA Bases with Naphthalene and Graphene. *Journal of Chemical Theory and Computation* **2013**, *9*, 2090–2096.

(46) Vovusha, H.; Sanyal, S.; Sanyal, B. Interaction of Nucleobases and Aromatic Amino Acids with Graphene Oxide and Graphene Flakes. *The Journal of Physical Chemistry Letters* **2013**, *4*, 3710–3718.

(47) Enyashin, A. N.; Gemming, S.; Seifert, G. DNA-wrapped carbon nanotubes. *Nanotechnology* **2007**, *18*, 245702.

(48) Stepanian, S.; Karachevtsev, M.; Glamazda, A.; Karachevtsev, V.; Adamowicz, L. Stacking interaction of cytosine with carbon nanotubes: MP2, DFT and Raman spectroscopy study. *Chemical Physics Letters* **2008**, *459*, 153–158.

(49) Shukla, M.; Dubey, M.; Zakar, E.; Namburu, R.; Czyznikowska, Z.; Leszczynski, J. Interaction of nucleic acid bases with single-walled carbon nanotube. *Chemical Physics Letters* **2009**, *480*, 269–272.

(50) Akdim, B.; Pachter, R.; Day, P. N.; Kim, S. S.; Naik, R. R. On modeling biomolecular–

surface nonbonded interactions: application to nucleobase adsorption on single-wall carbon nanotube surfaces. *Nanotechnology* **2012**, *23*, 165703.

(51) Ramraj, A.; Hillier, I. H.; Vincent, M. A.; Burton, N. A. Assessment of approximate quantum chemical methods for calculating the interaction energy of nucleic acid bases with graphene and carbon nanotubes. *Chemical Physics Letters* **2010**, *484*, 295–298.

(52) Umadevi, D.; Sastry, G. N. Quantum Mechanical Study of Physisorption of Nucleobases on Carbon Materials: Graphene versus Carbon Nanotubes. *The Journal of Physical Chemistry Letters* **2011**, *2*, 1572–1576.

(53) Sarmah, A.; Roy, R. K. Understanding the Interaction of Nucleobases with Chiral Semiconducting Single-Walled Carbon Nanotubes: An Alternative Theoretical Approach Based on Density Functional Reactivity Theory. *The Journal of Physical Chemistry C* **2013**, *117*, 21539–21550.

(54) Chehel Amirani, M.; Tang, T.; Cuervo, J. Quantum mechanical treatment of binding energy between DNA nucleobases and carbon nanotube: A DFT analysis. *Physica E: Low-dimensional Systems and Nanostructures* **2013**, *54*, 65–71.

(55) Chehel Amirani, M.; Tang, T. A QM:MM model for the interaction of DNA nucleotides with carbon nanotubes. *Phys. Chem. Chem. Phys.* **2015**, *17*, 7564–7575.

(56) Frischknecht, A. L.; Martin, M. G. Simulation of the Adsorption of Nucleotide Monophosphates on Carbon Nanotubes in Aqueous Solution. *The Journal of Physical Chemistry C* **2008**, *112*, 6271–6278.

(57) Lehninger, A.; Nelson, D.; Cox, M. *Lehninger Principles of Biochemistry*; W. H. Freeman, 2005; Chapter 8.

(58) Boghaei, D. M.; Gharagozlou, M. Charge transfer complexes of adenosine-5′-monophosphate and cytidine-5′-monophosphate with water-soluble cobalt(II) Schiff base

complexes in aqueous solution. *Spectrochimica Acta Part A: Molecular and Biomolecular Spectroscopy* **2006**, *63*, 139 – 148.

(59) Frisch, M. J. et al. Gaussian 09 Revision A.1. Gaussian Inc. Wallingford CT 2009.

(60) Lindahl, E.; Hess, B.; van der Spoel, D. GROMACS 3.0: a package for molecular simulation and trajectory analysis. *Molecular modeling annual* **2001**, *7*, 306–317.

(61) Bayly, C. I.; Cieplak, P.; Cornell, W.; Kollman, P. A. A well-behaved electrostatic potential based method using charge restraints for deriving atomic charges: the RESP model. *The Journal of Physical Chemistry* **1993**, *97*, 10269–10280.

(62) Case, D. et al. AmberTools13. University of California, San Francisco 2012.

(63) Barone, V.; Cossi, M. Quantum Calculation of Molecular Energies and Energy Gradients in Solution by a Conductor Solvent Model. *The Journal of Physical Chemistry A* **1998**, *102*, 1995–2001.

(64) Pullman, A.; Pullman, B. Molecular electrostatic potential of the nucleic acids. *Quarterly Reviews of Biophysics* **1981**, *14*, 289–380.

(65) Pullman, A.; Pullman, B.; Lavery, R. Molecular electrostatic potential versus field. significance for DNA and its constituents. *Journal of Molecular Structure: THEOCHEM* **1983**, *93*, 85 – 91, Proceedings of the XIIIth Congress of Theoretical Chemists of Latin Expression.

(66) P, P.; R, L. P.; K, J. Molecular electrostatic potential versus field. significance for DNA and its constituents. *Environmental Health Perspectives* **1985**, *61*, 191–202.

(67) Das, A.; Sood, A.; Maiti, P. K.; Das, M.; Varadarajan, R.; Rao, C. Binding of nucleobases with single-walled carbon nanotubes: Theory and experiment. *Chemical Physics Letters* **2008**, *453*, 266–273.

(68) Vaart, A. v. d.; Merz, K. M., Jr. Charge transfer in biologically important molecules: comparison of high-level ab initio and semiempirical methods. *International Journal of Quantum Chemistry* **2000**, *77*, 27–43.

(69) Maksić, Z.; Ángyán, J. *Theoretical Treatment of Large Molecules and Their Interactions*; International Series in Heat and Mass Transfer; Springer-Verlag, 1991.

(70) Lu, J.; Nagase, S.; Zhang, X.; Wang, D.; Ni, M.; Maeda, Y.; Wakahara, T.; Nakahodo, T.; Tsuchiya, T.; Akasaka, T.; Gao, Z.; Yu, D.; Ye, H.; Mei, W. N.; Zhou, Y. Selective Interaction of Large or Charge-Transfer Aromatic Molecules with Metallic Single-Wall Carbon Nanotubes:Critical Role of the Molecular Size and Orientation. *Journal of the American Chemical Society* **2006**, *128*, 5114–5118, PMID: 16608346.

(71) Leenaerts, O.; Partoens, B.; Peeters, F. M. Adsorption of $H_2O$, $NH_3$, CO, $NO_2$, and NO on graphene: A first-principles study. *Phys. Rev. B* **2008**, *77*, 125416.